5294–5305 *Nucleic Acids Research, 2020, Vol. 48, No. 10* *Published online 5 May 2020*
doi: 10.1093/nar/gkaa319

Emergence of a novel immune-evasion strategy from an ancestral protein fold in bacteriophage Mu

Shweta Karambelkar [1,2,*], Shubha Udupa[1], Vykuntham Naga Gowthami[1], Sharmila Giliyaru Ramachandra[1], Ganduri Swapna[1] and Valakunja Nagaraja [1,2,*]

[1]Department of Microbiology and Cell Biology, Indian Institute of Science, Bangalore 560012, India and [2]Jawaharlal Nehru Centre for Advanced Scientific Research, Bangalore 560064, India

Received January 07, 2020; Revised April 17, 2020; Editorial Decision April 17, 2020; Accepted April 21, 2020

ABSTRACT

The broad host range bacteriophage Mu employs a novel 'methylcarbamoyl' modification to protect its DNA from diverse restriction systems of its hosts. The DNA modification is catalyzed by a phage-encoded protein Mom, whose mechanism of action is a mystery. Here, we characterized the co-factor and metal-binding properties of Mom and provide a molecular mechanism to explain 'methylcarbamoyl'ation of DNA by Mom. Computational analyses revealed a conserved GNAT (GCN5-related N-acetyltransferase) fold in Mom. We demonstrate that Mom binds to acetyl CoA and identify the active site. We discovered that Mom is an iron-binding protein, with loss of $Fe^{2+/3+}$-binding associated with loss of DNA modification activity. The importance of $Fe^{2+/3+}$ is highlighted by the colocalization of $Fe^{2+/3+}$ with acetyl CoA within the Mom active site. Puzzlingly, acid-base mechanisms employed by >309,000 GNAT members identified so far, fail to support methylcarbamoylation of adenine using acetyl CoA. In contrast, free-radical chemistry catalyzed by transition metals like $Fe^{2+/3+}$ can explain the seemingly challenging reaction, accomplished by collaboration between acetyl CoA and $Fe^{2+/3+}$. Thus, binding to $Fe^{2+/3+}$, a small but unprecedented step in the evolution of Mom, allows a giant chemical leap from ordinary acetylation to a novel methylcarbamoylation function, while conserving the overall protein architecture.

INTRODUCTION

In the ever-escalating arms race against bacteria, phages appear to be edging out their hosts by engineering a number of strategies (1,2). For example, phage Mu has evolved an immune-evasion strategy in the form of a unique and broadly protective DNA modification. The methylcarbamoyladenine modification or ncm^6A, confers resistance to >20 diverse restriction enzymes, enabling Mu to invade multiple bacterial hosts in addition to *Escherichia coli* (3–7) (Figure 1A). ncm^6A is unique to Mu, being found in no other viral or cellular life form. Decades after its discovery, little is known about the modification. Overexpression of Mom, the phage protein catalyzing the DNA modification, is lethal to *E. coli* (8,9). The toxicity also explains why phage Mu limits *mom* expression to a brief period in late lytic infection, after phage DNA replication is completed and the host is destined to die (10). DNA modification by Mom enables dramatically higher (up to 10^4 fold) efficiencies of plating compared to Mu *mom*$^-$ phages on restricting strains of *E. coli* (4). Owing to the selective advantage, numerous host- and phage-encoded proteins have evolved to regulate the potentially lethal *mom* gene in diverse ways (4,10,11). While intricate details surrounding *mom* gene regulation have been teased apart, the biochemistry of Mom and molecular mechanisms underlying the modification are still shrouded in mystery. Moreover, the absence of structurally or functionally characterized homologs of Mom has precluded confident bioinformatic prediction of the enzymatic requirements of Mom and the chemistry behind the biosynthesis of this unusual, bulky DNA modification (12). Here, we present the first successful isolation and characterization of Mom, including the discovery of its active site, metal-binding properties and co-factor requirements. A combination of computational, biochemical and mutational analyses reveals a collaboration between acetyl CoA and $Fe^{2+/3+}$ for accomplishing the unusual modification. Based on these findings, we explain how phage Mu may have evolved a novel recipe for immune-evasion using ancient molecular ingredients.

*To whom correspondence should be addressed. Tel: +91 80 23600668; Fax: +91 80 23602697; Email: vraj@iisc.ac.in
Correspondence may also be addressed to Shweta Karambelkar. Email: shwetak@alum.iisc.ac.in

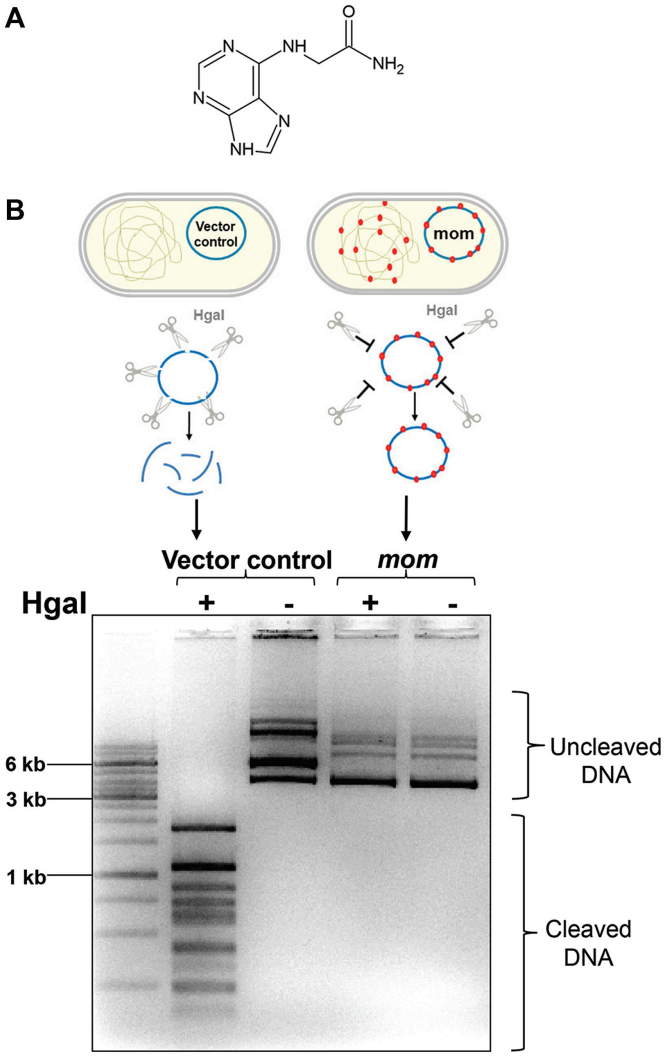

Figure 1. DNA modification activity of Mom. (**A**) Structure of the modified base N^6-methylcarbamoyl adenine. (**B**) Analysis of the *in vivo* DNA modification activity of Mom using the restriction endonuclease HgaI. Plasmid DNA was isolated from *E. coli* C41(DE3) cells harbouring the empty vector (vector control) or expressing Mom. DNA modification is depicted by red dots in the schematic. To examine if cellular DNA was modified by Mom, 1 μg plasmid DNA was digested with HgaI and products were analyzed on a 1% agarose ethidium bromide gel. While plasmids from vector control cells get digested into expected sized products, plasmids from *mom*-expressing cells remain unaffected by HgaI.

MATERIALS AND METHODS

Reagents, strains and plasmids

All chemicals used in the study were procured from Sigma, unless otherwise stated. The *E. coli* strains, primers and plasmids used in the study are described in Supplementary data Tables S1–S3 and Supplementary Figure S1. Detailed methods describing the purification and characterization of Mom, HPLC–MS^n analysis of the Mom-modified nucleoside, genetic and biochemical screens to identify Mom interactors, ferrozine assay, etc. are provided in the supplementary information.

Cloning and mutagenesis of *mom*

Phage Mu *mom* was ligated into the BamHI site of pVN6, a modification of the T7 expression vector pET11d (13,14). A regulatory plasmid pNC1, derived from pLysE, served to express T7 lysozyme and minimize leaky expression (13). Plasmid pVN6*mom* was used as a template for the generation of *mom* mutants. Mutations were introduced by site-directed mutagenesis using inverse PCR with adjacent non-overlapping primers, with forward primers harboring the desired mutation (15).

Analysis of *in vivo* activity of Mom

Escherichia coli C41(DE3) cultures harboring the regulatory plasmid pNC1 and the wild type or mutant *mom* plasmids were grown at 37°C to mid exponential phase and induced with 0.5 mM IPTG. Incubation was continued for 12 h at 16°C. Alternately, when using the pBAD expression system for *mom* expression, *E. coli* cultures harbouring the wild type or mutant *mom* plasmids were grown to mid log phase and induced with a final concentration of 0.2% arabinose. Incubation was continued overnight at 37°C. Plasmid DNA was isolated from the cultures using Qiagen miniprep kits and 1 μg DNA was digested with HgaI (2 units/μl, NEB). Products were analyzed on a 1% agarose ethidium bromide gel.

In silico prediction of structure and co-factor of Mom

The amino acid sequence of Mom was submitted to various structure prediction servers such as Robetta (16) and I-TASSER (17) available online at http://www.robetta.org/submit.jsp, http://zhanglab.ccmb.med.umich.edu/I-TASSER/, respectively. The modeled structures of Mom were submitted to the COFACTOR server available online at http://zhanglab.ccmb.med.umich.edu/COFACTOR/ in order to model the Mom-acetyl CoA complex, obtain functional insights including ligand-binding site, gene-ontology terms and enzyme classification derived from the best functional homology template. Models were visualized and analyzed using The PyMOL Molecular Graphics System, Version 2.0 Schrödinger, LLC. or the UCSF Chimera software available online at http://www.cgl.ucsf.edu/chimera (18). 3D co-ordinates of the modeled Mom-acetyl CoA complex are provided in Supplementary Figure S2. The structure of the N- and C-termini of Mom is difficult to reliably predict owing to lack of counterparts in template structures and so residues 1–28 and 195–231 have not been depicted in the model (12).

Analysis of thermostability of Mom in the presence of ligands

Purified Mom (12 μM) in HEPES buffer (10 mM HEPES–NaOH (pH 7.4), 14.33 mM β-mercaptoethanol, 100 mM or 300 mM NaCl) was incubated with ligand for 5 min on ice followed by 10 min at room temperature. Reactions (10 μl each) were set up in duplicates, loaded into nanoDSF grade glass capillaries and placed into Prometheus NT.48 (NanoTemper Technologies). A linear thermal ramp

(1°C/min, 20–80°C) was applied and the thermal unfolding of Mom was monitored by detecting the temperature-dependent change in tryptophan fluorescence at emission wavelengths of 330 and 350 nm. Protein melting points (T_m) were calculated from the first derivative of the ratio of tryptophan emission intensities at 330 and 350 nm by the Prometheus NT.Control software.

Binding affinity quantifications using microscale thermophoresis (MST)

Affinity measurements of purified Mom with various ligands were carried out on a Monolith NT.115 instrument (NanoTemper Technologies GmbH). Mom was fluorescently labeled using NanoTemper's Protein Labeling Kit RED-NHS or RED-tris-NTA dye (for his-tagged Mom and mutants). Ligands including acetyl CoA, *S*-adenosyl methionine (SAM), coenzyme A (CoASH), malonyl coenzyme A and salts of various metal ions were resuspended or dissolved in MST buffer (10 mM HEPES–NaOH (pH 7.4), 300 mM NaCl and 14 mM β-mercaptoethanol) to prepare a 16 step two-fold dilution series. Diluted ligands were incubated with 50 nM of labeled Mom at room temperature for 5 min and reactions were spun at 17000g for 5 min. Supernatants were loaded into NanoTemper premium coated capillaries. MST measurements were performed at 25°C using 60% MST power and 90% LED power. Data analyses were carried out using NanoTemper analysis software.

RESULTS

Expression and activity assay for Mom

Isolation of Mom remained elusive in the past owing to protein toxicity (8) and insolubility upon overexpression in *E. coli* (9). To successfully express Mom in a soluble form, we deployed a tightly regulated, dual plasmid pET expression system developed previously (13). Mom-modified DNA from phage Mu-infected hosts is known to be resistant to at least 20 restriction endonucleases, including HgaI, PvuII and SalI, to which unmodified DNA is sensitive (6). Taking cue from this, we developed a convenient and robust assay for detecting Mom activity. To determine whether Mom, overexpressed using the pET system, was proficient at modifying DNA *in vivo*, we isolated plasmid DNA from cells expressing Mom and treated it with the restriction endonuclease HgaI. While DNA from vector-control cells was completely digested to the expected cleavage products, DNA from cells that expressed Mom remained undigested, indicating that expressed Mom is functional *in vivo* (Figure 1B). Similar results were obtained with PvuII and SalI digestion of plasmid DNA isolated from Mom-expressing cells (Supplementary Figure S3). Furthermore, single point mutations in Mom (described in later sections) abolish the resistance to HgaI, indicating that protection from HgaI is specific to Mom activity.

Properties of Mom

Having confirmed the activity of Mom *in vivo*, we next attempted to isolate Mom. Hexahistidine-tagged Mom purified by Ni-NTA chromatography precipitated upon removal of imidazole. Hence, we designed an alternate ion-exchange-based protocol for purifying Mom in a soluble form (Supplementary Figures S4A and B). The molecular mass of untagged Mom, analyzed by LC–ESI-MS, matched the expected mass of 27050 Da and revealed that the N-terminal methionine encoded by the gene is absent (Supplementary Figure S4C). The far-UV CD spectrum of Mom showed that it has appreciable secondary structure comprised of approximately 13% alpha helices and 19% beta sheets (Supplementary Figure S4D). The fluorescence spectrum of the protein contained an expected red shift and a change in emission intensity upon chemical denaturation (Supplementary Figure S4E), indicating that in the native state the protein is folded with some buried tryptophan residues. Surface plasmon resonance studies showed that Mom binds to DNA with an affinity of ∼0.2 nM (Supplementary Figure S4F). In addition, analytical gel filtration and glutaraldehyde cross-linking experiments indicated that Mom exists as a dimer in solution (Supplementary Figures S4G and H). Having successfully expressed functionally active Mom and characterized its properties, we set out to understand its enigmatic enzyme function.

Acetyltransferase fold in Mom

Given that no structurally or functionally characterized homologs of Mom exist, we subjected the sequence of Mom to *de novo* and threading-based structure-prediction tools Robetta and I-TASSER, respectively. Both of the disparate structure-prediction methods revealed an evolutionary relationship between Mom and the GCN5-related N-acetyltransferase (GNAT) superfamily, as reported previously (12) (Figure 2). The analyses predict a classic GNAT fold occupying the core of Mom, with extensions at the N- and C-termini (Figure 2). The GNAT fold of Mom is comprised of a central, highly curved beta sheet sandwiched between five alpha helices. In addition to the overall fold, Mom displays several GNAT-like structural features, including the classic splayed beta strands β4 and β5 and a resultant V-shaped cleft for binding of acyl coenzyme A (19) (Figure 2). Given the structural similarity with acetyltransferases, the COFACTOR server predicted acetyl CoA, the co-factor most commonly utilized by the GNAT superfamily, as the co-factor of Mom (Figure 2). As in prototypical acetyltransferases, acetyl CoA in the Mom-acetyl CoA model fitted into the structurally conserved V-shaped cleft of Mom, adopting a characteristic 'bent' conformation (Figure 2), again suggesting acetyl CoA as the co-factor of Mom (20).

Mom binds to acetyl CoA

To test if Mom interacts with acetyl CoA, we employed differential scanning fluorimetry, which detects changes in the melting temperature (Tm) of a target protein upon interaction with a ligand (21,22). Interaction between Mom and acetyl CoA was evident from the dose-dependent effect of acetyl CoA on the Tm of Mom (Figure 3A and Supplementary Table S4). In contrast, no such effect was observed with compounds like S-adenosyl methionine (SAM), NAD^+, glycine, ATP, etc. (Figure 3B and Supplementary

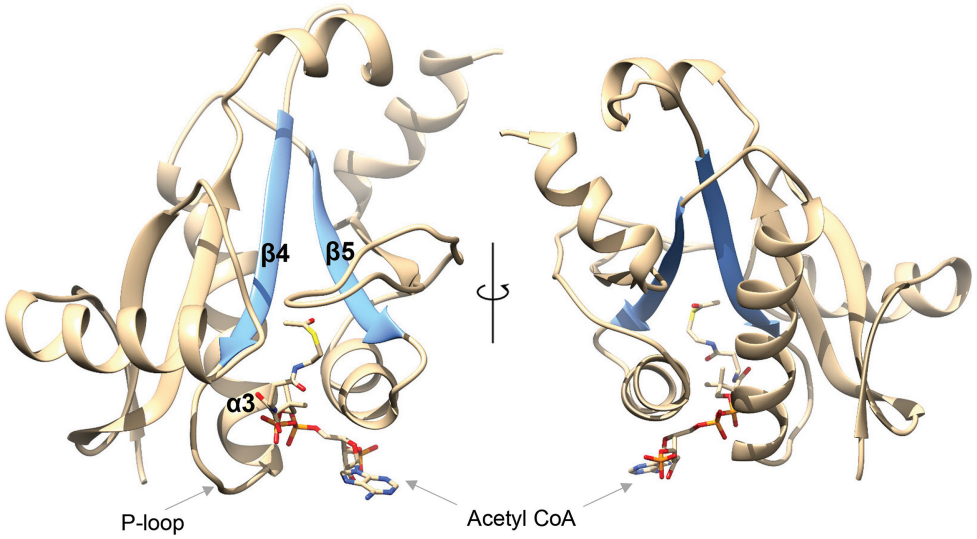

Figure 2. Mom is structurally related to acetyltransferases. Mom harbors a classic GNAT fold in its core, as revealed by disparate structure prediction methods. The fold comprises a six-stranded curved beta sheet sandwiched between five alpha helices. The beta sheet is largely antiparallel; the only exception being strands β4 and β5 (highlighted in blue), a structural feature conserved in the GNAT superfamily. β4 and β5 splay apart towards their C-termini, forming an inverted V-shaped cleft (blue), likely occupied by acetyl CoA, the co-factor most commonly employed by the GNAT superfamily, bound in a characteristic bent conformation. In addition, Mom harbors the P-loop and the βαβ (β4-α3-β5) motif, structural elements critical for generating the acetyl CoA-binding site in the GNAT fold, as indicated (19). As in prototypical GNAT structures, the pyrophosphate binding loop or P-loop of Mom appears poised to form direct or water-mediated hydrogen bonds to the pyrophosphate arm of acetyl CoA, while the backbone of β4 interacts intimately with the pantothenate arm of acetyl CoA via hydrogen bonds.

Table S4). A decrease in the Tm of Mom upon binding to acetyl CoA indicated that the interaction results in a more flexible or open protein conformation. A comparable effect was also observed with coenzyme A, a by-product of acyl CoA hydrolysis. Longer CoA derivatives exhibited weaker or no interaction with Mom (Supplementary Table S4). Such a preference for acetyl CoA over longer coenzyme A derivatives is displayed by other acetyl CoA-utilizing GNAT members as well (23). We next quantified the Mom-acetyl CoA interaction using microscale thermophoresis, which measures biomolecular interactions by monitoring the motion of molecules along microscopic temperature gradients, detecting ligand-induced changes in the hydration shell, charge, or size of macromolecules (24,25). While Mom bound to acetyl CoA with $K_d \sim 49\ \mu M$, no detectable interaction was observed with the control ligand *S*-adenosyl methionine (Figure 3C).

Mom catalyzes methylcarbamoyl transfer, not acetyl transfer

Based on the structural resemblance of Mom to acetyltransferases and its ability to bind acetyl CoA, it was tempting to hypothesize that Mom functioned as a prototypical acetyltransferase. However, Mom is known to transfer an unusual methylcarbamoyl ($–CH_2CONH_2$) group rather than acyl group (–COR, such as acetyl ($–COCH_3$), propionyl ($–COC_2H_5$), etc.) typically transferred by acetyltransferases (3,19). To confirm that the modification was indeed ncm^6A and not some acylated form of adenine, we revisited the original study by Swinton *et al.* (3). To do so, genomic DNA from *E. coli* cells expressing Mom was digested to nucleosides and analyzed using LC–ESI/MS^n (Supplementary Figure S5 and Supplementary Table S5). In the *mom*$^+$ samples, we observed a unique species (MomdA), with mass corresponding to ncm^6dA (methylcarbamoyldeoxyadenosine), accompanied by reduced levels of unmodified deoxyadenosine (dA) (Supplementary Figures S5A and B). Furthermore, collision-induced dissociation of MomdA yielded fragments diagnostic of ncm^6dA (Supplementary Figures S5C and D), thus reaffirming the identity of the modification. The fragmentation data ruled out acetyl($–COCH_3$)adenine and glycyl($–COCH_2NH_2$)adenine (identical mass as ncm^6A), conceivable with known GNAT chemistries employing acetyl CoA and glycyl tRNA, respectively (19,26). Having confirmed the chemical nature of the modification, we next sought to understand how Mom could accomplish the methylcarbamoyl transfer.

Exploring conventional and unconventional chemistries to decipher Mom mechanism

Acetyl CoA participates as a two-carbon donor by donating its acetyl group, engaging via the acetyl moiety's carbonyl carbon (e.g. GNAT mechanisms) or methyl carbon (e.g. condensation reactions) (20,27). As stated before, GNAT mechanisms support transfer of acetyl moiety ($-COCH_3$) to adenine, but not of $–CH_2COR$ (R being –OH or $–NH_2$) required for ncm^6A (20). On the other hand, condensation reactions can transfer $–CH_2COR$ group to electrophilic acceptors but not to nucleophilic acceptors like the N^6 amino group of adenine (27). This is because condensation involves deprotonation of the methyl group of acetyl CoA, which renders the carbon nucleophilic and thus non-reactive with the nucleophilic N^6 amino group of adenine (Supplementary Figure S6A) (27). In other words, no conventional mechanism supports acetyl CoA as the co-factor

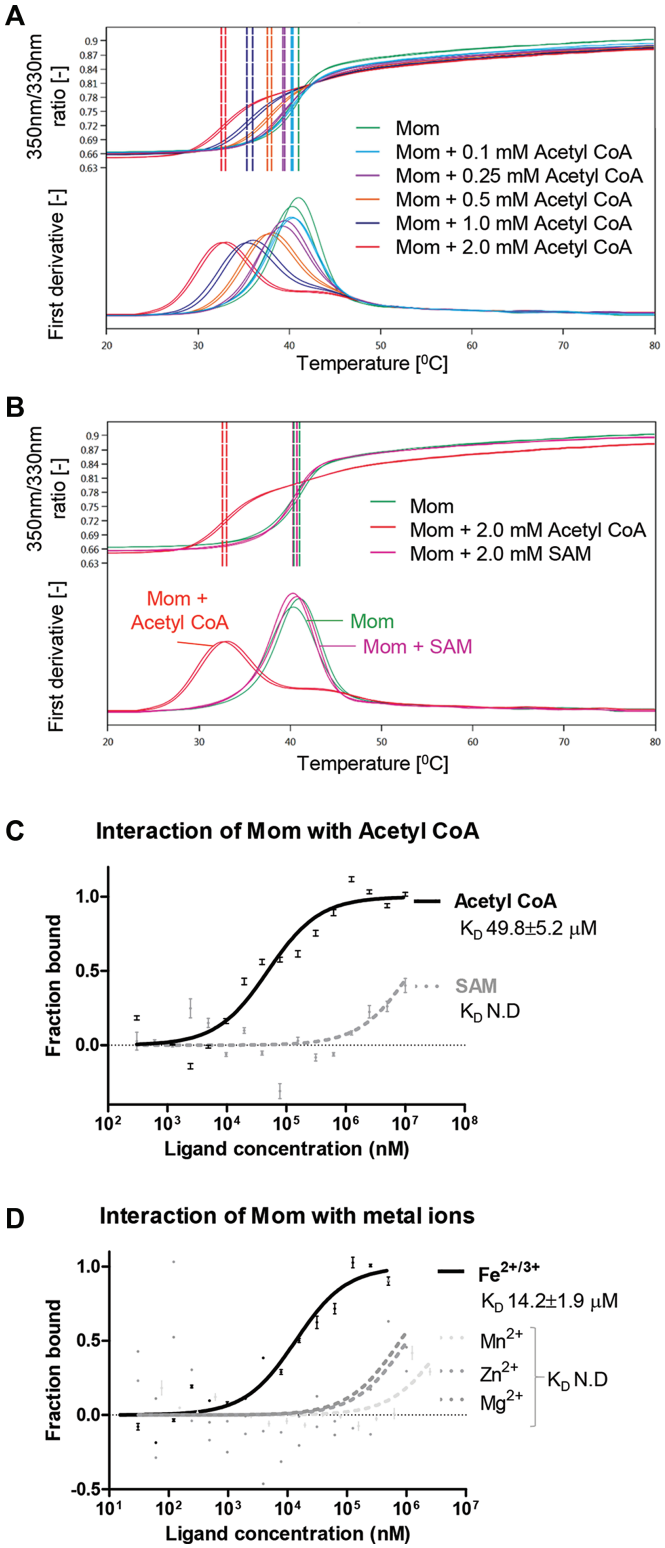

Figure 3. Interaction of Mom with acetyl CoA and other ligands. (**A**) Dose-dependent effect of acetyl CoA on the thermostability of Mom. Mom was incubated with indicated concentrations of acetyl CoA and subjected to thermal ramp (1°C/min, 20–80°C). The shift in the intrinsic tryptophan fluorescence of Mom upon temperature-induced unfolding was monitored by detecting the emission fluorescence at 330 and 350 nm. Protein melting points (Tm) were determined from the transition midpoints (dotted vertical lines in the upper panel) corresponding to peaks in the first derivatives of the 350/330 fluorescence data (lower panel). Reactions were carried out in duplicates. (**B**) Comparison of thermostability of Mom in the presence of acetyl CoA and SAM. Representative thermal denaturation curves of Mom alone (green), Mom incubated with 2 mM acetyl CoA (red) and Mom incubated with 2 mM SAM (magenta). While SAM has no detectable effect on the thermostability of Mom, acetyl CoA significantly destabilizes Mom. Reactions were carried out in duplicates. (**C**) Quantification of the binding affinity of Mom with acetyl coenzyme A using microscale thermophoresis. Mom was fluorescently labeled and titrated against indicated concentrations of ligands. Normalized fluorescence is plotted for analysis of thermophoresis. Data were fitted using the law of mass action to determine dissociation constants (K_D). Data shown are representative of three independent experiments. Error bars represent standard deviations of $n = 3$ measurements. Acetyl CoA interacts with Mom while SAM shows undetectable interaction. (**D**) Specificity of Mom-iron interaction. Microscale thermophoresis was carried out using fluorescently labeled Mom and various divalent metal ions and data plotted as described for Figure 3C. While $Fe^{2+/3+}$ interacts with Mom, Mn^{2+}, Zn^{2+} and Mg^{2+} showed undetectable interaction. Metal ions Ca^{2+}, Co^{2+} and Cu^{2+} also failed to interact with Mom (data could not be fitted).

of Mom. So, we broadened our investigation and examined other potential co-factors and mechanisms for methylcarbamoylation of adenine.

Given that our *in vivo* assays demonstrated that methylcarbamoylation of DNA *in vivo* required no phage gene apart from Mom (Figure 1B), it was reasonable to hypothesize that the co-factor used by Mom must be a host-derived metabolite. We searched the *E. coli* metabolome database for molecules wherein a good leaving group is attached to the methylcarbamoyl moiety, thus favoring a direct nucleophilic attack from the substrate amine of adenine (28). However, no such donor candidate could be found, making the possibility of a single-step reaction unlikely. Next, we examined the involvement of potential two-carbon donors, such as glyoxylate and cx-SAM, a carboxylated derivative of S-adenosyl-L-methionine which donates methylcarboxyl group (–CH_2COOH) to hydroxyuridine in tRNA modification reactions (29,30). However, Mom activity remained unaffected in strains lacking glyoxylate or the cx-SAM synthetic machinery (Supplementary Figure S6B), thus ruling out their participation in the Mom reaction.

While ncm^6A is unique to phage Mu DNA, a similar modification ncm^5U is common in archaeal and eukaryotic tRNA (31). Strikingly, Elp3 - the enzyme catalyzing the ncm^5U modification, also harbors an acetyl CoA-binding GNAT domain (32,33). Additionally, Elp3 contains a radical SAM (rSAM) domain harbouring a 4Fe–4S cluster and S-adenosyl methionine (SAM) (33,34). A highly reactive 'acetyl CoA radical' produced by the rSAM domain attacks the substrate uridine, forming an adduct whose hydrolysis and amidation yield ncm^5U (31,33). Although Mom lacks a rSAM domain, the presence of an acetyl CoA-binding GNAT domain hinted at an Elp3-like free radical-based mechanism for Mom. Given that some rSAM enzymes utilize trans-encoded rSAM domains (35,36), we hypothesized that Mom recruited a host-encoded rSAM domain. We tested this possibility by checking the ability of Mom to modify DNA in various *E. coli* strains lacking rSAM genes. An exhaustive search of the *E. coli* genome yielded 67 experimentally validated or predicted genes encoding 4Fe–4S clusters typical of rSAM proteins. Surprisingly, Mom ac-

tivity was detected in all 67 rSAM single gene knock-outs, indicating that none was necessary for Mom function and rendering them unlikely partners of Mom (Supplementary Figure S6C and Supplementary Table S1).

Investigating genetic interactions of *mom* with the host

Next, we undertook an unbiased genome-wide approach to identify host genes or co-factors involved in Mom activity. Multi-step reactions, often catalyzed by multi-protein complexes, alleviate the need for 'one-step donors' of bulky chemical moieties (29,32,37–39). Hence, we examined using both genetic and biochemical approaches, the possibility of Mom interacting with host protein(s). The genetic approach entailed expression of the toxic Mom protein in random transposon mutagenesis libraries of *E. coli*, followed by selection for survivors (Supplementary Figures S6D and E). Survival, despite Mom overexpression, would indicate compromised Mom function, possibly due to disruptive insertions in genes encoding the co-factor synthesis machinery or putative interacting partner(s) of Mom. However, the survivors we obtained from the assay either bore deletions in the *mom* gene or seemed to retain *mom* and the DNA modification while overcoming toxicity in unknown ways. Bacterial survivors that were mom^+ and yet defective for DNA modification could not be isolated even after multiple attempts, suggesting the essentiality of or redundancy in the genes participating in the Mom modification pathway.

Host protein interactions reveal Mom as an iron-binding protein

We next undertook a more direct biochemical approach to reveal host factors required for the modification. In a protein-protein interaction assay to capture interacting partners of Mom from *E. coli* cell extracts, we recovered ferritin and subunits of the pyruvate dehydrogenase (PDH) complex (Supplementary Figure S7). Ferritin is an iron storage protein of *E. coli* involved in supplying iron atoms to iron-binding proteins and Fe-S cluster biosynthesis proteins (40,41), whereas the PDH complex is central to acetyl CoA biosynthesis (42). These results not only returned our attention to acetyl CoA, but also revived the possibility of a radical-based mechanism for the participation of acetyl CoA in the Mom reaction. Fe^{2+} and other transition metal ions (Mn^{2+}, Cu^{2+}, Co^{2+}, etc.) in many metalloproteins generate highly reactive substrate radicals (43,44). The association of Mom with the iron-supplying protein, ferritin, as suggested by the pull-down assay, prompted us to check if Mom was an iron-binding protein. Indeed, the colorimetric ferrozine assay revealed intrinsically bound $Fe^{2+/3+}$ in Mom (Supplementary Figure S8A–D). Furthermore, microscale thermophoresis experiments showed that Mom binds specifically to iron and to no other divalent metal ions tested, including Mn^{2+}, Cu^{2+}, Mg^{2+}, Co^{2+}, Zn^{2+} and Ca^{2+} (Figure 3D). In retrospect, the presence of intrinsically bound iron in Mom was also indicated by the pale brown color of the purified Mom protein, with an absorption peak at 540 nm observed in addition to that at 280 nm (Supplementary Figure S8E).

Given the well-known role of $Fe^{2+/3+}$ in generating free radicals and accomplishing seemingly prohibitive reactions, we hypothesized a plausible scheme of reactions for Mom (Figure 4) (45,46). Briefly, oxidation of acetyl CoA catalyzed by Fe^{2+} would generate a glyoxylic acid ester of coenzyme A, which forms a Schiff base with N^6 amine of adenine. Reduction of the Schiff base would transfer the activated carboxymethyl ($–CH_2COSCoA$) group to adenine, and its amidation can yield ncm^6A (Figure 4). Lack of knowledge of additional host factors or reaction conditions required, if any, have precluded *in vitro* reconstitution of the Mom reaction. Supplementing the reactions with alpha-ketoglutarate and ascorbate, commonly employed as reductants by $Fe^{2+/3+}$-utilizing dioxygenases, or adding whole or fractionated cell extracts failed to show any effect (47). Nevertheless, having observed specific interactions of Mom with acetyl CoA and $Fe^{2+/3+}$ *in vitro*, we hypothesized that mechanisms involving acetyl CoA as the two-carbon donor and iron as a catalyst require the two reactants to be in physical proximity within the active site of Mom. We thus sought to characterize the active site of Mom by identifying and disrupting the binding sites of acetyl CoA and $Fe^{2+/3+}$ and examining the effects on Mom activity.

Indispensability of acetyl CoA and $Fe^{2+/3+}$ for Mom function

Mom homologs (numerous uncharacterized proteins annotated as Mom owing to sequence similarity with phage Mu Mom) from various representative genera were aligned to identify conserved residues (Supplementary Figure S9). Alanine substitutions at conserved polar residues impaired the activity of Mom to different extents, as demonstrated by the endonuclease protection assay employed in the previous sections (Figure 5A and Supplementary Figure S10). Subsequently, each of the six functionally compromised point mutants was purified and individually tested for defects in $Fe^{2+/3+}$ and/or acetyl CoA-binding using microscale thermophoresis assay (Figure 5B). The mutants fell into four categories based on defects in (i) acetyl CoA-binding only (H48A and S114A), (ii) both iron- and acetyl CoA-binding (Y49A and Y149A), (iii) iron-binding only (D139A) and (iv) neither iron-binding nor acetyl CoA-binding (R101A) (Figure 5B). These functionally important residues mapped to the acetyl CoA cleft in Mom, suggesting the region to be the active site of Mom (Figure 5C). Conversely, mutating a poorly conserved residue located far from the acetyl CoA cleft (e.g. L69) did not perturb Mom activity (Figures 5A and Supplementary Figure S9). Mutagenesis data further validated the relatedness between Mom and the GNAT superfamily predicted *in silico*. In GNAT members, acetyl CoA mainly contacts the protein via backbone interactions (20). The only few conserved side chain contacts include a tyrosine in α4 (Y149 in Mom), which stabilizes the acetyl arm of acetyl CoA, and a serine in α3 (S114 in Mom), which stabilizes the pyrophosphate arm of CoA (19,20). S114 and Y149 appear to furnish similar roles in Mom, evident from their conservation across Mom homologs (Supplementary Figure S9) and mutations therein impairing both acetyl CoA binding and DNA modification activity of Mom (Figures 5A–C). Surprisingly, mutation of Y149 also abolished iron binding (Figure 5B). Defects in iron-binding and DNA modification were also seen with mutations in residues Y49 and D139, which along with Y149, likely co-ordinate an

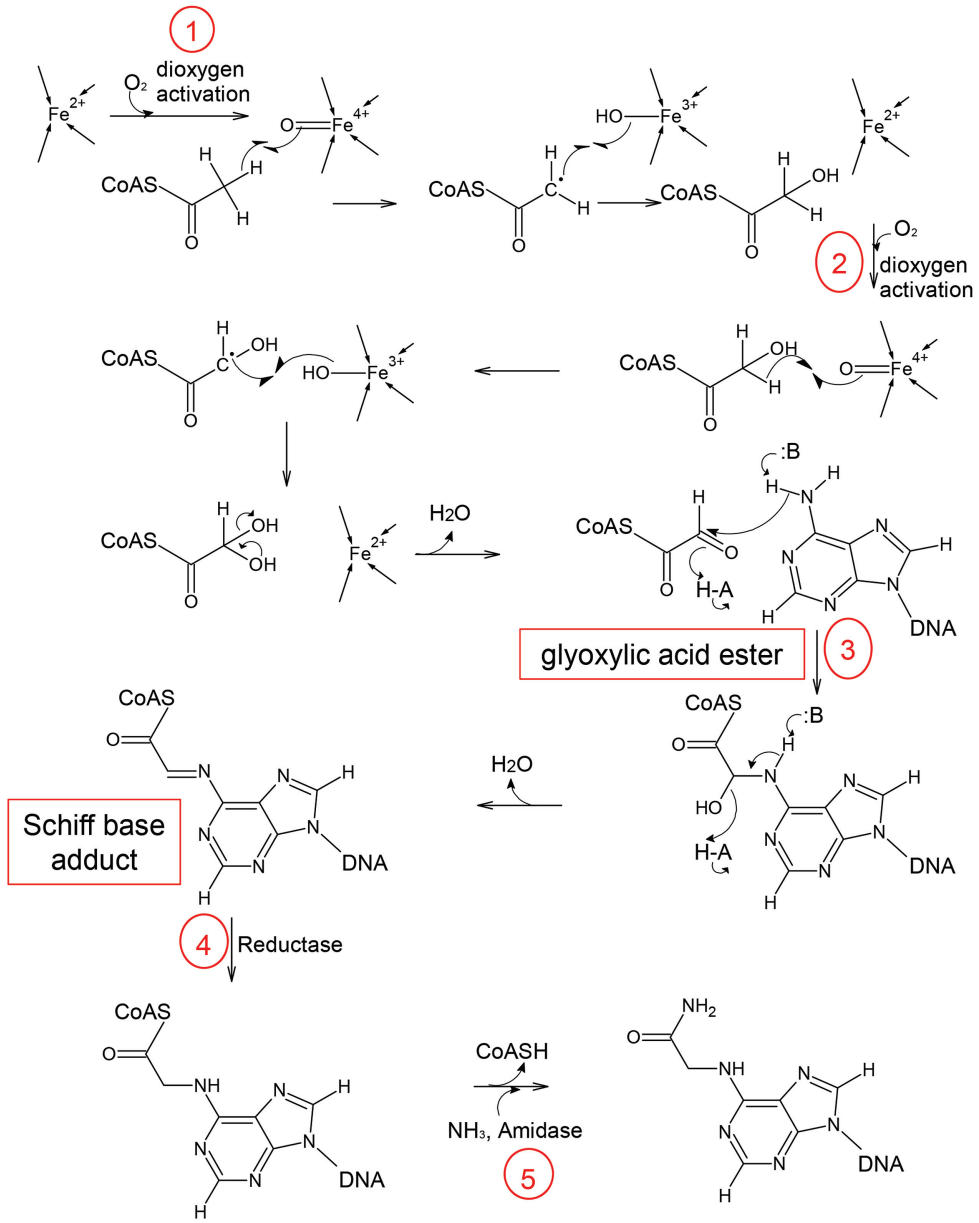

Figure 4. Proposed pathway for $Fe^{2+/3+}$ ion-catalyzed methylcarbamoylation of adenines by Mom. Reiterative oxidation of the methyl group of acetyl CoA with molecular oxygen (indicated by reactions 1 and 2), catalyzed by Fe^{2+} bound in the Mom active site, generates an aldehyde group (glyoxylic acid ester) capable of forming a Schiff base with the substrate amine of adenine in DNA (reaction 3). Reduction of the Schiff base transfers the carboxymethyl ($–CH_2COSCoA$) group to adenine (reaction 4). Amidation of this activated carboxymethyl group results in the final methylcarbamoyl ($-CH_2CONH_2$) modification (reaction 5). B-unidentified general base, HA-unidentified general acid.

$Fe^{2+/3+}$ ion (Figures 5A–C and Supplementary Figure S10). Remarkably, the putative iron-coordinating triad maps near the acetyl group of acetyl CoA modeled within the Mom active site (Figure 5C). This explains why mutating iron-coordinating tyrosines 49 and 149 also impairs acetyl CoA binding (Figure 5B and C). The converse however is not true, with residue S114, which stabilizes acetyl CoA via the pyrophosphate arm at a region far from the active site, having no effect on iron-binding (Figure 5B and C). Interestingly, residues like Y149, long conserved for their GNAT-specific roles (19), seem co-opted for a novel task of iron-binding in Mom (Figure 5B). Notably, the $Fe^{2+/3+}$-coordinating residues appear sub-optimally spaced in the Mom active site. However, conformational changes induced by binding of ligands $Fe^{2+/3+}$ and acetyl CoA, evident from the shifts in the melting temperature of Mom, likely bring the residues closer (Figure 3A and Supplementary Figure S11).

R101, a functionally critical residue in Mom is conserved amongst Mom homologs but not across the GNAT superfamily (Figure 5A and Supplementary Figure S9) (12). R101 maps within the active site cleft of Mom, being located near the acetyl moiety of acetyl CoA (Figure 5C and D). Surprisingly, although mutation of R101 totally abolished

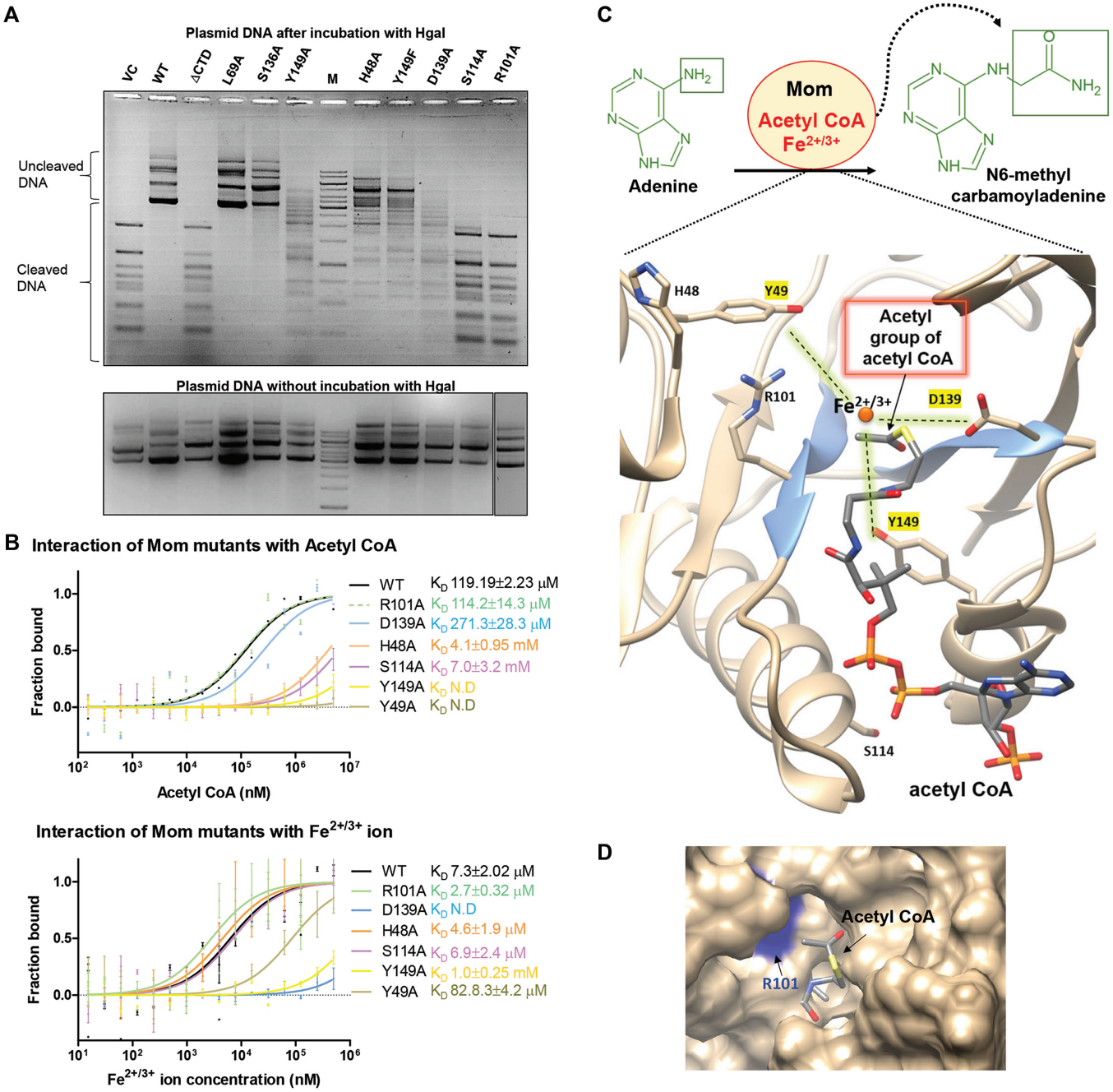

Figure 5. DNA modification activity and co-factor-interactions of Mom mutants. (**A**) Analysis of *in vivo* DNA modification activity of Mom mutants. Plasmid DNA was isolated from *E. coli* C41(DE3) cells expressing wild type or mutant Mom proteins, as indicated. VC denotes vector control and ΔCTD denotes a 175 aa long Mom construct with 56 residues from the C-terminus deleted. M represents 1kb ladder. 1 μg DNA was digested with the restriction endonuclease HgaI and products were analyzed on a 1% agarose ethidium bromide gel. Different mutations exert variable degrees of effects on the activity of Mom, with S114 and R101A compromising Mom activity most severely. Lower panel shows the undigested plasmids corresponding to those in the upper panel. (**B**) Co-factor-binding defects in Mom mutants analyzed using microscale thermophoresis. His-tagged wild-type Mom (WT) and mutants were fluorescently labeled and titrated against indicated concentrations of ligands acetyl CoA (upper panel) and $Fe^{2+/3+}$ (lower panel). Normalized fluorescence is plotted for analysis of thermophoresis. Data were fitted using the law of mass action to determine dissociation constants (K_D). Data shown are representative of three independent experiments. Error bars represent standard deviations of n = 3 measurements. All mutants except R101A and D139A are defective in acetyl CoA binding, whereas Y49A, D139A and Y149A are compromised for $Fe^{2+/3+}$ binding. (**C**) Active site of Mom. Residues found to be important for the DNA modification activity of Mom (side chains shown) map onto the active site pocket of Mom, with the splayed strands β4 and β5 which form the acetyl CoA-binding cleft colored blue. A $Fe^{2+/3+}$ ion is colocalized near the acetyl arm of acetyl CoA within the active site of Mom. The tentative location of the $Fe^{2+/3+}$ ion is depicted based on mutagenesis data, with residues critical for $Fe^{2+/3+}$-binding highlighted. (**D**) R101 residue of Mom. Of all the point mutations introduced in the Mom active site, the effect of R101A substitution was the most detrimental to the modification activity, despite having no effect on acetyl CoA- and $Fe^{2+/3+}$-binding. The active site cleft viewed from the acetyl end of acetyl CoA shows the acetyl group emerging into a grove, likely to be the substrate adenine-binding cleft. The residue R101 is positioned at the opening of the cleft and appears poised for substrate recognition.

Mom activity (Figure 5A), binding to acetyl CoA and iron was not affected (Figure 5B). Consistent with its location in the active site and positioning near the opening of the acetyl CoA cleft and substrate-binding cleft (Figure 5D), R101 possibly is involved in DNA base recognition or stabilization rather than acetyl CoA- or iron-binding. A flipped adenine base in DNA could enter the active site, placing itself near the acetyl group of acetyl CoA. The DNA substrate may additionally be stabilized by other residues on the surface of Mom, besides R101. The C-terminal region of Mom is highly basic (Supplementary Figure S1B) and likely to harbor DNA-binding residues, but its structure could not be modeled due to lack of counterparts in GNAT templates.

In a nutshell, the computational prediction of a GNAT fold in Mom was experimentally validated by (i) binding of acetyl CoA to Mom (Figure 3), (ii) conservation of GNAT fold-specific residues (Y149 and S114) and their fulfilment of predicted roles in acetyl CoA binding (Supplementary Figure S9 and Figure 5B) (19,20), (iii) loss of DNA modification activity upon mutagenesis of GNAT-specific conserved residues (Figure 5A), (iv) preference of Mom for acetyl CoA over other CoA esters like propionyl CoA, succinyl CoA, etc., similar to other acetyl CoA-utilizing members of the GNAT superfamily (Supplementary Table S4), (v) clustering of conserved residues in the acetyl CoA cleft or putative active site of Mom (Figure 5C) and (vi) loss of DNA modification activity and co-factor interactions of Mom upon mutation of putative active site residues (Figures 5A and B). Overall, computation-guided biochemical analyses reveal the active site of Mom as a milieu in which the acetyl group of acetyl CoA, $Fe^{2+/3+}$ and substrate adenine come together to perform an unusual DNA modification reaction (Figure 4 and 5C). In contrast to acetyl CoA, which is well-known to occupy a conserved cleft in the GNAT fold (19), binding of both—iron and DNA to acetyltransferases, to our knowledge, is totally unprecedented. Our data reveals that the GNAT-like active site of Mom has retained ancestral GNAT features while gaining at least two novel functions- iron-binding and utilization of DNA as a substrate. Moreover, colocalization of iron and acetyl group in the active site of Mom, together with data from mutagenesis of the amino acid residues involved in their binding, supports the catalytic role of iron suggested by the plausible molecular mechanism presented in Figure 4.

DISCUSSION

In this report, we have addressed a long-standing question about the mechanism of the unusual DNA modification in phage Mu. Inability to express tightly regulated, highly toxic Mom in recombinant form had hampered the understanding of its function and the reaction pathway for 'methylcarbamoylation' of adenosines in Mu genome. In addition to successfully purifying Mom, we discover $Fe^{2+/3+}$ and acetyl CoA as interacting co-factors and propose their catalytic roles and novel functions in the GNAT active site. While these findings advance our understanding of the catalytic path followed by Mom, demonstration of its *vitro* enzymatic activity has eluded all attempts so far. We anticipate that description of the challenges and our attempts to demonstrate the activity of Mom *in vitro,* together with the reaction mechanism proposed would form a primer for future mechanistic studies on Mom.

While conventional chemistry fails to explain acetyl CoA as a co-factor of Mom, a radical-based mechanism can explain it, for instance, through oxidation of acetyl CoA (Figure 4). Our detailed investigation renders several other metabolites and pathways unlikely, leaving an iron-mediated radical mechanism the most plausible one for methylcarbamoylation of adenine. Although co-localization of functionally important residues with $Fe^{2+/3+}$ and acetyl CoA within the putative active site of Mom supports a catalytic role, *in vitro* DNA modification assays, elusive so far, are needed to validate their role in catalysis. From our studies, it is apparent that besides acetyl CoA and $Fe^{2+/3+}$, host factors, both small molecules and proteins, would be required for ncm^6A biosynthesis. Given that Mom is the only phage-encoded protein necessary for the modification, reducing agents or electron sources, amidases, reductases, and so on are likely to be derived from the host rather than from Mu (Figure 4). Besides, apart from the GNAT fold, Mom exhibits no known enzymatic signatures in its sequence or structure, rendering its direct involvement in steps like amidation or Schiff base reduction unlikely. Although our transposon mutagenesis studies failed to identify any host factors, biochemical pull-down assays detected iron storage protein ferritin and acetyl CoA-producing pyruvate dehydrogenase complex interacting with Mom. The findings not only illustrate how phages strike at the host's metabolic machinery and resources, but also convey the power of protein-protein interaction studies to throw light on the workings of enzymes. Further investigation along these lines may reveal more interactors and help fill the gaps in our knowledge and reveal details underlying the reaction. Nevertheless, the discovery of acetyl CoA and iron in the Mom active site unravels a concrete piece in the enigmatic DNA modification puzzle. Our findings pave the way for further mechanistic studies, potential harnessing of the modification for therapeutic application of phages, and more.

Use of acetyl CoA as a cofactor by Mom appears to be an evolutionarily stable strategy, given that acetyl CoA is ubiquitous and abundant, with concentrations in exponentially dividing *E. coli* reaching ~0.6 mM (48). Mu expresses Mom only briefly at the end of lytic infection, and cellular acetyl CoA pools are unlikely to be a limiting factor for Mom activity (8,49). Moreover, the central metabolic role of acetyl CoA precludes the host from dispensing with it in order to thwart DNA modification by Mom.

While simple 'methylation' appears to be the modification of choice for most nucleic acid modification systems, nature has, albeit less frequently, explored other more complex modifications (38,50). Their biological roles often extend beyond providing immunity against restriction enzymes (1,4,6,51) to those concerning regulation of gene expression (base J in trypanosomes (52,53), hydroxymethylcytosine (54)), protein synthesis (e.g. tRNA anti-codon loop modifications (55–58)), and structural and thermal stability of nucleic acids (59–61). Biosynthetic pathways underlying various nucleic acid modifications besides phage Mu ncm^6A have long remained enigmatic. Recently, chemistries behind some complex modifications have begun to be unraveled

(31,38,50,62,63). Examples include radical SAM enzyme-mediated reactions on RNA (31,46) and Tet1-catalyzed hydroxylation and subsequent oxidation of methylcytosines in DNA (45,64,65). Notably, methylation of DNA was long thought to be too stable to be enzymatically removed, but it was subsequently found to be erasable via the action of widely occurring Tet family proteins (45). A property that unites extraordinary enzymes like radical SAM proteins and Tet1 dioxygenases is their ability to bind iron and catalyze free radical chemistries. Iron likely enables Mom to catalyze an unusual reaction using acetyl CoA instead of carrying out a reaction typical of the GNAT fold. We suggest that the occurrence of iron-mediated chemistry might be more common than previously thought and may be the missing piece in several other biological puzzles.

Summing up, phage Mu Mom represents evolutionary and chemical innovation at multiple levels. Mom is the first GNAT member to bind $Fe^{2+/3+}$ and carry out a non-acylation reaction on DNA, a substrate unexplored so far by the GNAT superfamily. The novelty of DNA as a GNAT substrate is noteworthy, given that the GNAT superfamily is known to modify a vast variety of biomolecules- proteins, peptides, sugars, RNA, antibiotics, etc. (19,20). From an evolutionary perspective, the metal-mediated ability to generate highly reactive radical species vastly expands the catalytic capabilities of a given structural scaffold (44). Thus, characterization of Mom unveils not only the catalytic versatility possible within the GNAT world, but also a novel class of enzymes whose chemistry lies outside the canonical borders of the GNAT superfamily. Evolutionary tinkering of enzyme active sites thus explains how a disproportionately high number of functions emerge from a small number of folds (66). As for phage Mu, the evolutionary accident of rebooting an ancestral enzyme fold enables it to successfully penetrate the anti-phage arsenal of its bacterial hosts.

SUPPLEMENTARY DATA

Supplementary Data are available at NAR Online.

ACKNOWLEDGEMENTS

We are grateful to Karl Drlica for critical reading of the manuscript, and thank P. Balaram, K.R. Prasad, Debasisa Mohanty, Amrita Hazra, J. Gowrishankar, D.N. Rao, Umesh Varshney, S. Mahadevan, B. Gopal, Raghavan Varadarajan, Ujjwal Rathore, Souvik Bhattacharyya and members of the Nagaraja laboratory for scientific input and discussions. We thank Ashish Rangra, Samata Chaudhuri, and Rahul Pramjeet for technical help, Shubhada for bioinformatics support, Sunita and Srilatha from the Department of Biotechnology-supported mass spectrometry and Biacore facilities, respectively, at the Indian Institute of Science for technical assistance, and Saji Menon and Sivaramaiah Nallapeta of Nanotemper technologies for their assistance with microscale thermophoresis and nanoDSF measurements.

Author contributions: S.K. and V.N. designed research; S.K., S.U., V.N.G., S.G.R. and G.S. performed research; S.K. and V.N. analyzed data; and S.K. and V.N. wrote the paper.

FUNDING

V.N. is a J. C. Bose Fellow of the Department of Science and Technology, Government of India. S.K. was supported by fellowship from the Council of Scientific and Industrial Research, India, and post-doctoral fellowship of Jawaharlal Nehru Centre for Advanced Scientific Research. This research was supported by various grants to V.N. from the Department of Science and Technology, Government of India, Indian Institute of Science - Department of Biotechnology, Government of India partnership program, and Life science research, education and training at JNCSAR [BT/INF/22/SP27679/2018]. The open access publication charge for this paper has been waived by Oxford University Press – *NAR* Editorial Board members are entitled to one free paper per year in recognition of their work on behalf of the journal.

Conflict of interest statement. None declared.

REFERENCES

1. Labrie,S.J., Samson,J.E. and Moineau,S. (2010) Bacteriophage resistance mechanisms. *Nat. Rev. Microbiol.*, **8**, 317–327.
2. Vasu,K., Rao,D.N. and Nagaraja,V. (2019) *Reference Module in Life Sciences*. Elsevier.
3. Swinton,D., Hattman,S., Crain,P.F., Cheng,C.S., Smith,D.L. and McCloskey,J.A. (1983) Purification and characterization of the unusual deoxynucleoside, alpha-N-(9-beta-D-2′-deoxyribofuranosylpurin-6-yl)glycinamide, specified by the phage Mu modification function. *Proc. Natl Acad. Sci. U.S.A.*, **80**, 7400–7404.
4. Toussaint,A. (1976) The DNA modification function of temperate phage Mu-1. *Virology*, **70**, 17–27.
5. Hattman,S. (1979) Unusual modification of bacteriophage Mu DNA. *J. Virol.*, **32**, 468–475.
6. Kahmann,R. (1983) Methylation regulates the expression of a DNA-modification function encoded by bacteriophage Mu. *Cold Spring Harb. Symp. Quant. Biol.*, **47**, 639–646.
7. Kahmann,R. and Hattman,S. (1987) In Symonds,N., Toussaint,A., van de Putte,P. and Howe,M.M. (eds.), *Phage Mu*. Cold Spring Harbor Laboratory, Cold Spring Harbor, NY, pp. 93–109.
8. Hattman,S. and Ives,J. (1984) S1 nuclease mapping of the phage Mu *mom* gene promoter: a model for the regulation of *mom* expression. *Gene*, **29**, 185–198.
9. Kahmann,R., Seiler,A., Wulczyn,F.G. and Pfaff,E. (1985) The *mom* gene of bacteriophage Mu: a unique regulatory scheme to control a lethal function. *Gene*, **39**, 61–70.
10. Hattman,S. (1999) Unusual transcriptional and translational regulation of the bacteriophage Mu *mom* operon. *Pharmacol. Ther.*, **84**, 367–388.
11. Karambelkar,S., Swapna,G. and Nagaraja,V. (2012) Silencing of toxic gene expression by Fis. *Nucleic Acids Res.*, **40**, 4358–4367.
12. Kaminska,K.H. and Bujnicki,J.M. (2008) Bacteriophage Mu Mom protein responsible for DNA modification is a new member of the acyltransferase superfamily. *Cell Cycle*, **7**, 120–121.
13. Chandrashekharan,S., Paul,B.D. and Nagaraja,V. (1998) Design of a novel regulatory circuit for expression of restriction endonucleases. *Biol. Chem.*, **379**, 579–582.
14. Balke,V., Nagaraja,V., Gindlesperger,T. and Hattman,S. (1992) Functionally distinct RNA polymerase binding sites in the phage Mu *mom* promoter region. *Nucleic Acids Res.*, **20**, 2777–2784.
15. Jain,P.C. and Varadarajan,R. (2014) A rapid, efficient, and economical inverse polymerase chain reaction-based method for generating a site saturation mutant library. *Anal. Biochem.*, **449**, 90–98.
16. Kim,D.E., Chivian,D. and Baker,D. (2004) Protein structure prediction and analysis using the Robetta server. *Nucleic Acids Res.*, **32**, W526–W531.

17. Yang,J., Yan,R., Roy,A., Xu,D., Poisson,J. and Zhang,Y. (2015) The I-TASSER Suite: protein structure and function prediction. *Nat. Methods*, **12**, 7–8.
18. Pettersen,E.F., Goddard,T.D., Huang,C.C., Couch,G.S., Greenblatt,D.M., Meng,E.C. and Ferrin,T.E. (2004) UCSF Chimera–a visualization system for exploratory research and analysis. *J. Comput. Chem.*, **25**, 1605–1612.
19. Salah Ud-Din,A.I., Tikhomirova,A. and Roujeinikova,A. (2016) Structure and functional diversity of GCN5-Related N-Acetyltransferases (GNAT). *Int. J. Mol. Sci.*, **17**, E1018.
20. Dyda,F., Klein,D.C. and Hickman,A.B. (2000) GCN5-related N-acetyltransferases: a structural overview. *Annu. Rev. Biophys. Biomol. Struct.*, **29**, 81–103.
21. Niesen,F.H., Berglund,H. and Vedadi,M. (2007) The use of differential scanning fluorimetry to detect ligand interactions that promote protein stability. *Nat. Protoc.*, **2**, 2212–2221.
22. Vivoli,M., Novak,H.R., Littlechild,J.A. and Harmer,N.J. (2014) Determination of protein-ligand interactions using differential scanning fluorimetry. *J. Vis. Exp.*, e51809.
23. Ringel,A.E. and Wolberger,C. (2016) Structural basis for acyl-group discrimination by human Gcn5L2. *Acta Crystallogr. D Struct. Biol.*, **72**, 841–848.
24. Parker,J.L. and Newstead,S. (2014) Molecular basis of nitrate uptake by the plant nitrate transporter NRT1.1. *Nature*, **507**, 68–72.
25. Seidel,S.A., Dijkman,P.M., Lea,W.A., van den Bogaart,G., Jerabek-Willemsen,M., Lazic,A., Joseph,J.S., Srinivasan,P., Baaske,P., Simeonov,A. *et al.* (2013) Microscale thermophoresis quantifies biomolecular interactions under previously challenging conditions. *Methods*, **59**, 301–315.
26. Benson,T.E., Prince,D.B., Mutchler,V.T., Curry,K.A., Ho,A.M., Sarver,R.W., Hagadorn,J.C., Choi,G.H. and Garlick,R.L. (2002) X-ray crystal structure of *Staphylococcus aureus* FemA. *Structure*, **10**, 1107–1115.
27. Kurz,L.C., Shah,S., Crane,B.R., Donald,L.J., Duckworth,H.W. and Drysdale,G.R. (1992) Proton uptake accompanies formation of the ternary complex of citrate synthase, oxaloacetate, and the transition-state analog inhibitor, carboxymethyl-CoA. Evidence that a neutral enol is the activated form of acetyl-CoA in the citrate synthase reaction. *Biochemistry*, **31**, 7899–7907.
28. Guo,A.C., Jewison,T., Wilson,M., Liu,Y., Knox,C., Djoumbou,Y., Lo,P., Mandal,R., Krishnamurthy,R. and Wishart,D.S. (2013) ECMDB: the *E. coli* metabolome database. *Nucleic Acids Res.*, **41**, D625–D630.
29. Kim,J., Xiao,H., Bonanno,J.B., Kalyanaraman,C., Brown,S., Tang,X., Al-Obaidi,N.F., Patskovsky,Y., Babbitt,P.C., Jacobson,M.P. *et al.* (2013) Structure-guided discovery of the metabolite carboxy-SAM that modulates tRNA function. *Nature*, **498**, 123–126.
30. Byrne,R.T., Whelan,F., Aller,P., Bird,L.E., Dowle,A., Lobley,C.M., Reddivari,Y., Nettleship,J.E., Owens,R.J., Antson,A.A. *et al.* (2013) S-Adenosyl-S-carboxymethyl-L-homocysteine: a novel cofactor found in the putative tRNA-modifying enzyme CmoA. *Acta Crystallogr. D. Biol. Crystallogr.*, **69**, 1090–1098.
31. Selvadurai,K., Wang,P., Seimetz,J. and Huang,R.H. (2014) Archaeal Elp3 catalyzes tRNA wobble uridine modification at C5 via a radical mechanism. *Nat. Chem. Biol.*, **10**, 810–812.
32. Huang,B., Johansson,M.J. and Bystrom,A.S. (2005) An early step in wobble uridine tRNA modification requires the Elongator complex. *RNA*, **11**, 424–436.
33. Glatt,S., Zabel,R., Kolaj-Robin,O., Onuma,O.F., Baudin,F., Graziadei,A., Taverniti,V., Lin,T.Y., Baymann,F., Seraphin,B. *et al.* (2016) Structural basis for tRNA modification by Elp3 from Dehalococcoides mccartyi. *Nat. Struct. Mol. Biol.*, **23**, 794–802.
34. Paraskevopoulou,C., Fairhurst,S.A., Lowe,D.J., Brick,P. and Onesti,S. (2006) The Elongator subunit Elp3 contains a Fe4S4 cluster and binds S-adenosylmethionine. *Mol. Microbiol.*, **59**, 795–806.
35. Ollagnier,S., Mulliez,E., Schmidt,P.P., Eliasson,R., Gaillard,J., Deronzier,C., Bergman,T., Graslund,A., Reichard,P. and Fontecave,M. (1997) Activation of the anaerobic ribonucleotide reductase from *Escherichia coli*. The essential role of the iron-sulfur center for S-adenosylmethionine reduction. *J. Biol. Chem.*, **272**, 24216–24223.
36. Kulzer,R., Pils,T., Kappl,R., Huttermann,J. and Knappe,J. (1998) Reconstitution and characterization of the polynuclear iron-sulfur cluster in pyruvate formate-lyase-activating enzyme. Molecular properties of the holoenzyme form. *J. Biol. Chem.*, **273**, 4897–4903.
37. van Leeuwen,F., Kieft,R., Cross,M. and Borst,P. (1998) Biosynthesis and function of the modified DNA base beta-D-glucosyl-hydroxymethyluracil in Trypanosoma brucei. *Mol. Cell. Biol.*, **18**, 5643–5651.
38. Weigele,P. and Raleigh,E.A. (2016) Biosynthesis and function of modified bases in bacteria and their viruses. *Chem. Rev.*, **116**, 12655–12687.
39. Mathews,C.K., Wheeler,L.J., Ungermann,C., Young,J.P. and Ray,N.B. (1993) Enzyme interactions involving T4 phage-coded thymidylate synthase and deoxycytidylate hydroxymethylase. *Adv. Exp. Med. Biol.*, **338**, 563–570.
40. Abdul-Tehrani,H., Hudson,A.J., Chang,Y.S., Timms,A.R., Hawkins,C., Williams,J.M., Harrison,P.M., Guest,J.R. and Andrews,S.C. (1999) Ferritin mutants of *Escherichia coli* are iron deficient and growth impaired, and fur mutants are iron deficient. *J. Bacteriol.*, **181**, 1415–1428.
41. Bitoun,J.P., Wu,G. and Ding,H. (2008) *Escherichia coli* FtnA acts as an iron buffer for re-assembly of iron-sulfur clusters in response to hydrogen peroxide stress. *Biometals*, **21**, 693–703.
42. Koike,M., Reed,L.J. and Carroll,W.R. (1960) alpha-Keto acid dehydrogenation complexes. I. Purification and properties of pyruvate and alpha-ketoglutarate dehydrogenation complexes of *Escherichia coli*. *J. Biol. Chem.*, **235**, 1924–1930.
43. Bollinger,J.M. Jr and Krebs,C. (2007) Enzymatic C-H activation by metal-superoxo intermediates. *Curr. Opin. Chem. Biol.*, **11**, 151–158.
44. Lewis,J.C., Coelho,P.S. and Arnold,F.H. (2011) Enzymatic functionalization of carbon-hydrogen bonds. *Chem. Soc. Rev.*, **40**, 2003–2021.
45. Tahiliani,M., Koh,K.P., Shen,Y., Pastor,W.A., Bandukwala,H., Brudno,Y., Agarwal,S., Iyer,L.M., Liu,D.R., Aravind,L. *et al.* (2009) Conversion of 5-methylcytosine to 5-hydroxymethylcytosine in mammalian DNA by MLL partner TET1. *Science*, **324**, 930–935.
46. Kimura,S. and Suzuki,T. (2015) Iron-sulfur proteins responsible for RNA modifications. *Biochim. Biophys. Acta*, **1853**, 1272–1283.
47. Hausinger,R.P. (2004) FeII/alpha-ketoglutarate-dependent hydroxylases and related enzymes. *Crit. Rev. Biochem. Mol. Biol.*, **39**, 21–68.
48. Takamura,Y. and Nomura,G. (1988) Changes in the intracellular concentration of acetyl-CoA and malonyl-CoA in relation to the carbon and energy metabolism of *Escherichia coli* K12. *J. Gen. Microbiol.*, **134**, 2249–2253.
49. Stoddard,S.F. and Howe,M.M. (1989) Localization and regulation of bacteriophage Mu promoters. *J. Bacteriol.*, **171**, 3440–3448.
50. Boccaletto,P., Machnicka,M.A., Purta,E., Piatkowski,P., Baginski,B., Wirecki,T.K., de Crecy-Lagard,V., Ross,R., Limbach,P.A., Kotter,A. *et al.* (2018) MODOMICS: a database of RNA modification pathways. 2017 update. *Nucleic Acids Res.*, **46**, D303–D307.
51. Bryson,A.L., Hwang,Y., Sherrill-Mix,S., Wu,G.D., Lewis,J.D., Black,L., Clark,T.A. and Bushman,F.D. (2015) Covalent modification of bacteriophage T4 DNA inhibits CRISPR-Cas9. *MBio*, **6**, e00648.
52. Reynolds,D., Cliffe,L., Forstner,K.U., Hon,C.C., Siegel,T.N. and Sabatini,R. (2014) Regulation of transcription termination by glucosylated hydroxymethyluracil, base J, in Leishmania major and Trypanosoma brucei. *Nucleic Acids Res.*, **42**, 9717–9729.
53. Borst,P. and Sabatini,R. (2008) Base J: discovery, biosynthesis, and possible functions. *Annu. Rev. Microbiol.*, **62**, 235–251.
54. Choi,I., Kim,R., Lim,H.W., Kaestner,K.H. and Won,K.J. (2014) 5-hydroxymethylcytosine represses the activity of enhancers in embryonic stem cells: a new epigenetic signature for gene regulation. *BMC Genomics*, **15**, 670.
55. Endres,L., Dedon,P.C. and Begley,T.J. (2015) Codon-biased translation can be regulated by wobble-base tRNA modification systems during cellular stress responses. *RNA Biol*, **12**, 603–614.
56. Gu,C., Begley,T.J. and Dedon,P.C. (2014) tRNA modifications regulate translation during cellular stress. *FEBS Lett.*, **588**, 4287–4296.
57. Agris,P.F. (1991) Wobble position modified nucleosides evolved to select transfer RNA codon recognition: a modified-wobble hypothesis. *Biochimie*, **73**, 1345–1349.
58. Agris,P.F., Eruysal,E.R., Narendran,A., Vare,V.Y.P., Vangaveti,S. and Ranganathan,S.V. (2017) Celebrating wobble decoding: Half a century and still much is new. *RNA Biol*, **15**, 537–553.

59. Kintanar,A., Yue,D. and Horowitz,J. (1994) Effect of nucleoside modifications on the structure and thermal stability of *Escherichia coli* valine tRNA. *Biochimie*, **76**, 1192–1204.
60. Lorenz,C., Lunse,C.E. and Morl,M. (2017) tRNA Modifications: Impact on structure and thermal adaptation. *Biomolecules*, **7**, E35.
61. Nomura,Y., Ohno,S., Nishikawa,K. and Yokogawa,T. (2016) Correlation between the stability of tRNA tertiary structure and the catalytic efficiency of a tRNA-modifying enzyme, archaeal tRNA-guanine transglycosylase. *Genes Cells*, **21**, 41–52.
62. Anton,B.P., Saleh,L., Benner,J.S., Raleigh,E.A., Kasif,S. and Roberts,R.J. (2008) RimO, a MiaB-like enzyme, methylthiolates the universally conserved Asp88 residue of ribosomal protein S12 in *Escherichia coli*. *Proc. Natl Acad. Sci. U.S.A.*, **105**, 1826–1831.
63. Lee,Y.J., Dai,N., Walsh,S.E., Muller,S., Fraser,M.E., Kauffman,K.M., Guan,C., Correa,I.R. Jr and Weigele,P.R. (2018) Identification and biosynthesis of thymidine hypermodifications in the genomic DNA of widespread bacterial viruses. *Proc. Natl Acad. Sci. U.S.A.*, **115**, E3116–E3125.
64. Kohli,R.M. and Zhang,Y. (2013) TET enzymes, TDG and the dynamics of DNA demethylation. *Nature*, **502**, 472–479.
65. Ito,S., Shen,L., Dai,Q., Wu,S.C., Collins,L.B., Swenberg,J.A., He,C. and Zhang,Y. (2011) Tet proteins can convert 5-methylcytosine to 5-formylcytosine and 5-carboxylcytosine. *Science*, **333**, 1300–1303.
66. Grant,A., Lee,D. and Orengo,C. (2004) Progress towards mapping the universe of protein folds. *Genome Biol.*, **5**, 107.